

# Time-of-Flight Mass Spectrometry With Latching Nb Meander Detectors

Brian V. Estey, James A. Beall, Gene C. Hilton, Kent D. Irwin, Dan R. Schmidt, Joel N. Ullom, and Robert E. Schwall

**Abstract**—Mass Spectrometry is widely used for protein characterization, structural virology, drug discovery, and clinical chemistry. However, the detection efficiency of existing detectors for mass spectrometry degrades rapidly as mass is increased, and is only  $\sim 10^{-5}$  at  $10^6$  Da. Superconducting detectors provide detection efficiency that is essentially independent of mass, and previous efforts have explored the use of superconducting tunnel junctions (STJs) and normal-insulator-superconductor (NIS) microcalorimeters as detectors. Both STJ and NIS detectors, however have active areas limited to  $\sim 1 \text{ mm}^2$ , well below the  $\sim 1 \text{ cm}^2$  required for a viable system. Microwave-interrogated microstripline meander detectors have the potential to provide the necessary area and speed. We describe such a design and present initial spectra of representative ionized biological molecules obtained from simple prototype detectors mounted on a cryocooler and interfaced to a commercial mass spectrometer.

**Index Terms**—Mass spectrometry, niobium meander.

## I. INTRODUCTION

**T**IME-OF-FLIGHT mass spectrometry is an important tool in the fields of analytical chemistry, biology, and material sciences [1]. More recently, clinical interest has developed in using the technique for screening antiviral drugs and differentiation of viral genomes. There is also demand by homeland security for rapid identification of pathogenic viruses [2]. These applications rely on the ability to analyse whole molecules with molecular masses on the order of  $10^6$  Daltons ( $1 \text{ Da} = 1$  atomic mass unit). Microchannel Plate (MCP) detectors, which are the standard for time-of-flight (TOF) mass spectrometry, have a detection efficiency that rapidly decreases with increasing molecular weight [3] and therefore are not suitable for these applications. Cryogenic detectors, on the other hand, have 100% efficiency for all molecular weights [4]–[6]. However, unlike previous cryogenic detectors, MCPs provide large detection area (up to 2.54 cm diameter) that enables the MCP to encompass the spread of biomolecules in the ion beam generated by a commercial spectrometer.

Manuscript received August 26, 2008. First published current version published July 10, 2009.

B. V. Estey was with the National Institute of Standards and Technology, Boulder, CO 80305 USA. He is now with the Department of Physics, University of California, Berkeley, CA 94720 USA (e-mail: estey@berkeley.edu).

J. A. Beall, G. C. Hilton, K. D. Irwin, D. R. Schmidt, J. N. Ullom and R. E. Schwall are with the National Institute of Standards and Technology, Boulder, CO 80303, USA (e-mail: schwall@boulder.nist.gov).

Color versions of one or more of the figures in this paper are available online at <http://ieeexplore.ieee.org>.

Digital Object Identifier 10.1109/TASC.2009.2018507

Prior work with cryogenic detectors has utilized superconducting tunnel junctions (STJs) [4], [5], [7] and normal-insulator-superconductor (NIS) microcalorimeters [8]. However, both STJs and NIS microcalorimeters require temperatures on the order of 100 mK and have areas limited to  $200 \mu\text{m} \times 200 \mu\text{m}$ . More recently there has been work done on superconducting stripline detectors using NbN meanders [9]. These detectors offer excellent rise-times, but the reset time is limited by the kinetic inductance [11] and hence the length of the meander. The limitation placed on the meander length by the kinetic inductance also restricts the detector area.

We describe here a microwave-interrogated Nb superconducting meander detector, which provides the rise-time advantages of the detector in [9] but with improved reset time. The superconducting meander detector is designed as a microstripline with controlled impedance, so that the reset time is not limited by the kinetic inductance. Thus the line can be made much longer, and the detector area can be much larger than that of a NbN meander detector.

We have divided the project into two parts: one effort is developing the microwave measurement system; the second, presented here, addresses system integration and the estimate of detector quantum efficiency relative to MCP's. For the system integration effort, we fabricated Nb superconducting meanders that are not microstripline. Nb was chosen rather than NbN for ease of fabrication since the objective of this work was system integration and proof of principle. This latching superconducting Nb meander detector does not rely on the kinetic inductance of the meander to reset the detector, and uses instead an external reset circuit. This allows the detector to be scaled to a larger size without affecting its response time. The microstripline-based meander utilizing microwave interrogation, is designed to be self resetting.

## II. MEANDER DETECTOR

A 100 nm niobium thin film was deposited on silicon substrate and a meander with a  $1 \mu\text{m}$  width was etched by use of photolithography (Fig. 1). Detectors ranging in size from  $(100 \mu\text{m})^2$  to  $(500 \mu\text{m})^2$  and linewidths of  $1.0 \mu\text{m}$  and  $1.5 \mu\text{m}$  were fabricated. The results presented here were obtained with a  $(500 \mu\text{m})^2$  meander having a linewidth of  $1.0 \mu\text{m}$  and fill factor of approximately 50%. When in operation, the detector is biased with a current of 28 mA at 3.4 K, 70% of the critical current (37 mA).

Unlike the kinetic inductance based meander [10], this detector has no intrinsic recovery mechanism. When a molecule impinges on the superconducting line, a hot spot is created that will expand through joule heating until the entire meander is

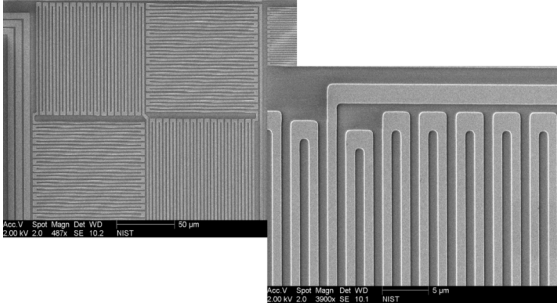


Fig. 1. SEM image of a  $200\ \mu\text{m} \times 200\ \mu\text{m}$  detector illustrating the  $1\ \mu\text{m}$  meander linewidth.

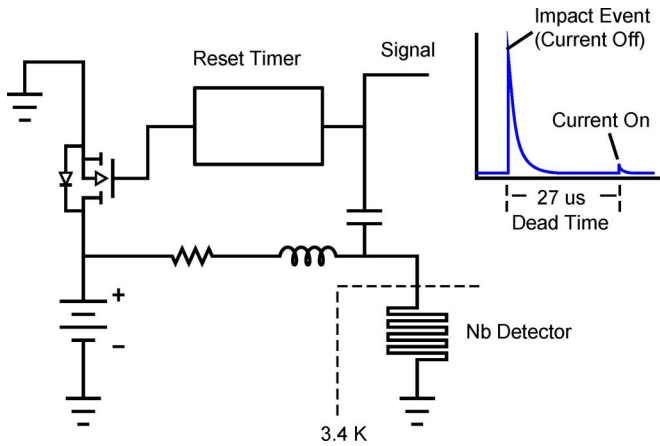


Fig. 2. Circuit diagram of the latching Nb meander detector and a representation of the signal output. The reset timer turns off the current to the detector by use of a high speed DMOS FET.

normal. Therefore a simple reset circuit is introduced to allow the Nb meander to relax back to its superconducting state. Fig. 2 shows the basic circuit design for the detector, where the reset timer turns off the current to the detector. This reset timer creates dead-time in data acquisition, which limits the detector's ability to record two separate events with similar molecular weights. The period required for the chip to return to the superconducting state is determined by the response time of the current switch and timer ( $\sim 1\ \mu\text{s}$ ). During this time, joule heating causes the temperature of the chip to increase well beyond its critical temperature, and  $\sim 27\ \mu\text{s}$  is required for the chip to cool below its transition temperature and reset.

The rise-time of the detector was measured to be  $\sim 9.8\ \text{ns}$  which is considerably slower than would be expected from calculations of the geometric and kinetic inductance [11] of this device. Our assumption is that this is due to stray impedance (primarily capacitance to ground) in the chip package, which was a simply designed printed circuit board. To verify this assumption, we measured the rise-time of a  $(200\ \mu\text{m})^2$  meander on the same chip. If the risetime was dominated by meander inductance, we would expect the risetime to decrease by approximately the ratio of the meander lengths or a factor of  $\sim 6$ . The measured rise-time for the  $(200\ \mu\text{m})^2$  meander is  $\sim 7.8\ \text{ns}$ , indicating that response time is dominated not by the detector but by stray impedance. As was expected, the smaller detector recorded fewer counts per spectrum when compared to the larger detector,



Fig. 3. Photographs of the integrated system with the cryostat bolted onto the MALDI-TOF mass spectrometer.

but otherwise functioned in an equivalent manner. Packaging for the microwave-interrogated detector is designed to minimize the effects of stray impedances.

### III. EXPERIMENT

#### A. Apparatus

The Nb meander was cooled by a commercial Gifford-McMahon (GM) cryocooler with an operating temperature of 3.4 K. The vacuum can of the cryocooler is attached to the flange of a commercial mass spectrometry workstation in place of the standard 2.54 cm diameter MCP detector. This allows the detectors to be exchanged with minimal effort. The total length of the flight tube with the cryogenic detector is approximately 1.3 meters, versus 1.1 meters with the standard MCP. The entire system is kept at a vacuum pressure of less than  $1.3 \times 10^{-5}\ \text{Pa}$  by the spectrometer's turbomolecular pump. The spectrometer is a linear TOF system that uses matrix-assisted laser desorption/ionization (MALDI-TOF) to ionize the sample (Fig. 3). The ions are accelerated through a potential difference  $V_0$  that imparts a kinetic energy

$$\frac{1}{2}mv^2 = e \cdot zV_0, \quad (1)$$

where  $V_0$  is the accelerating potential and  $e \cdot z$  is the ion charge. By measuring the arrival time of the ions at the detector, one is able to determine the  $m/z$  ratio for each molecule. An accelerating voltage of 25,000 V with a guide wire voltage of 70 V is used to collimate the beam and maximize the flux of larger ions to the detector. The accelerating voltage is turned on  $1.6\ \mu\text{s}$  after the laser pulse to allow collisions within the ion plume to reduce the effect of the initial ion velocity imparted by the ionization process.

Two samples were used to test the Nb meander detector, Bovine Serum Albumin (BSA) with a molecular weight of 66.4 kDa, and Immunoglobulin G (IgG) with a molecular weight of 142 kDa. A matrix solution was prepared from 0.1% Trifluoroacetic acid in water and Acetonitrile (7:3) mixed with Sinapinic acid to a concentration of 20 mg/ml. A solution of

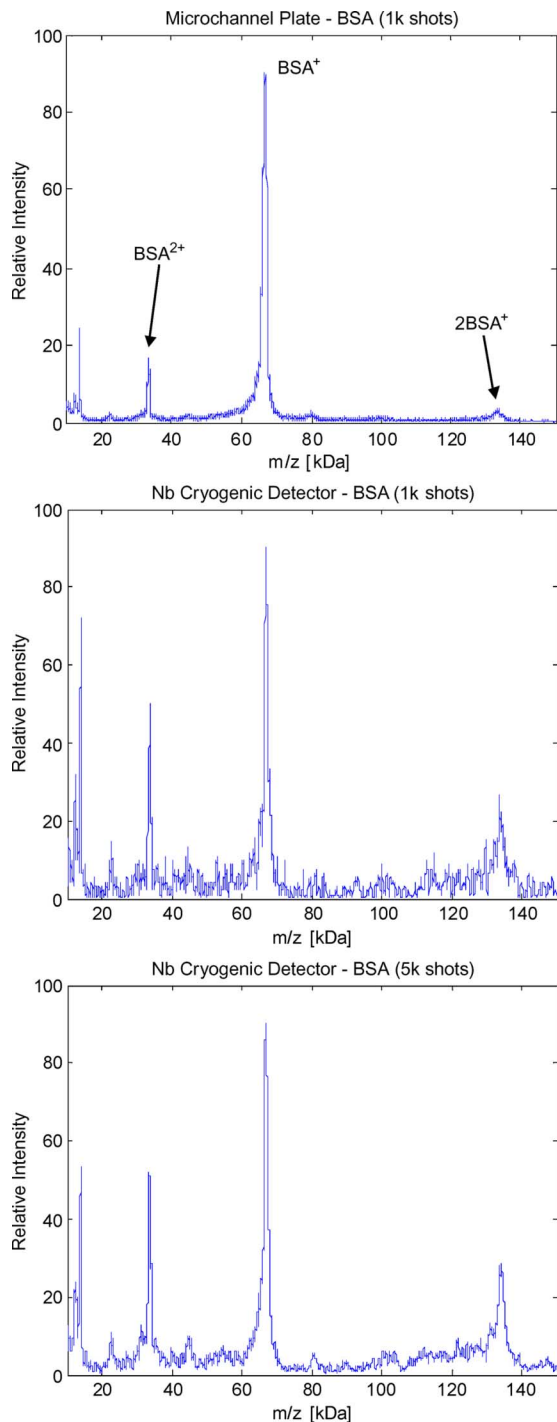


Fig. 4. BSA spectrum using the standard Microchannel Plate detector and the Nb meander detector.

BSA (10 mg/ml) or IgG (1.1 mg/ml) was mixed with the matrix solution at a ratio of 9:1, and an 8  $\mu$ l droplet of the final solution was deposited on the sample plate.

The biomolecule samples were ionized by a pulsed  $N_2$  laser. The output signal of the detector was routed into the digitizer of the mass spectrometry workstation and processed by the built-in electronics and software.

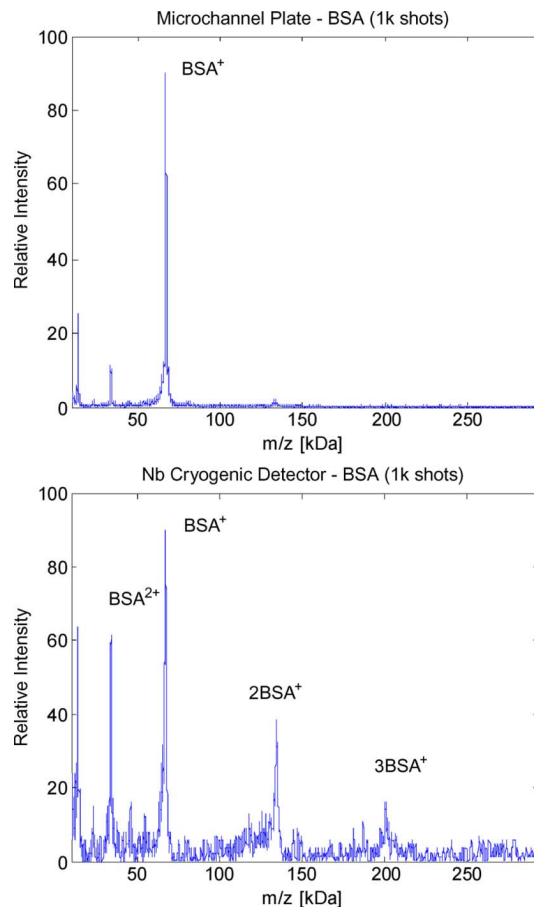


Fig. 5. Spectrum of BSA through the entire mass range of the spectrometer.

#### IV. RESULTS

Initial spectra were obtained with BSA. First the cryogenic detector was cooled to 3.4 K, where we recorded data from 1,000 and 5,000 laser pulses to obtain spectra. Then the detector was replaced by the MCP, and a spectrum of 1,000 laser shots was obtained from the same sample for comparison. The resulting mass per charge spectra can be seen in Fig. 4.

Quantitative comparison of the two detectors proved difficult, due to two primary factors. First, the area of the cryogenic detector is only  $\sim 1/2000$  that of the MCP, and hence it records fewer events for the same number of laser shots. Second, due to the dead time previously described, the cryogenic detector will fail to record a molecule arrival that occurs within 27  $\mu$ s of the arrival of a previous molecule. This means that the relative heights of peaks are not proportional to the relative abundance of incident ions. In particular, strong peaks such as  $BSA^+$  will be attenuated because the cryogenic detector can record a maximum of one count within the peak envelope for each laser shot.

It is possible, however, to draw some qualitative conclusions from the spectra by considering the peaks for the heavier ions. For example, because any ion impacting the cryogenic detector 27  $\mu$ s before the  $2BSA^+$  peak prevents the detection of this ion, the measured height of this peak could only be larger in the absence of the latching behavior. Therefore a comparison of the peak height to noise floor ratio for this ion for the two detectors will give a conservative estimate of the relative quantum efficiency; i.e. it can only underestimate the efficiency of the

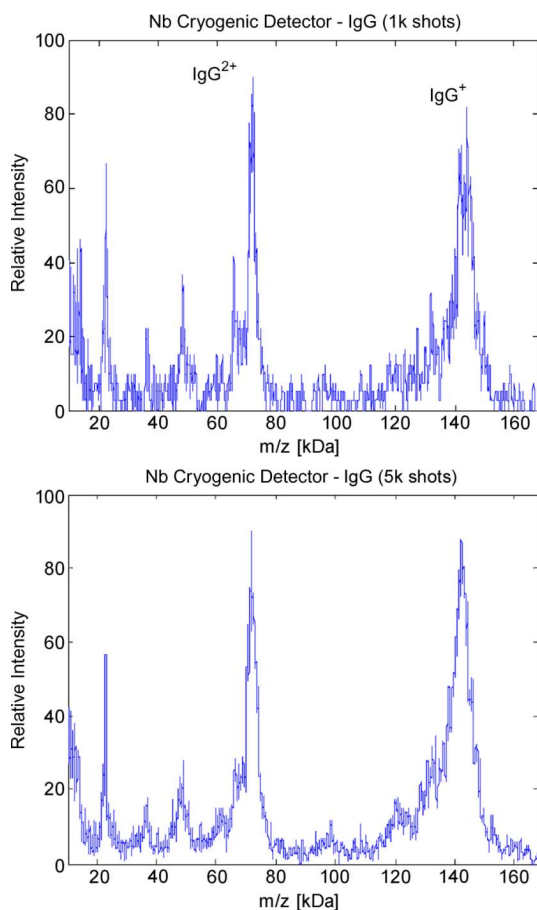


Fig. 6. IgG spectrum using the Nb meander detector.

cryogenic detector. The measured peak/noise ratio for  $2\text{BSA}^+$  peak in Fig. 4 is  $\sim 2.5\times$  larger for the cryogenic detector than for the MCP. Similarly, Fig. 5 shows a 1,000 laser shot spectrum obtained over the full mass range of the spectrometer. The peak/noise ratio of  $2\text{BSA}^+$  is again measured to be  $\sim 2.5$  greater for the cryogenic detector. In addition, the  $3\text{BSA}^+$  peak, which is not visible on the MCP, is clearly visible.

Fig. 6 presents data for a heavier molecule, IgG. Although the MALDI ionization process is less efficient for this material, we still obtain good signals for both the  $\text{IgG}^{2+}$  and  $\text{IgG}^+$  ions.

## V. MICROWAVE READOUT

As has been described previously [9]–[11], the reset time of a meander-type superconducting detector increases with the length of the meander, due to the kinetic inductance of the line. This causes detectors with areas approaching  $1\text{ cm} \times 1\text{ cm}$  to have reset times that are much longer than are required for high mass accuracy. In addition, the signal propagation time for meander detectors of this size with fill factor of 50% will be several hundred nanoseconds. This introduces a corresponding uncertainty in the arrival time of a molecule. These considerations are addressed by creating a controlled-impedance meander microstripline that is interrogated by an incident microwave signal at a multi-gigahertz frequency. Since the characteristic impedance (including kinetic inductance) of the microstripline is matched to the input and output circuits, the

kinetic inductance will not affect the recovery time. Furthermore, by measuring a reflected and transmitted microwave signal, it is possible to calculate the location on the meander of a molecule's impact, and hence the time at which the impact occurred, making it possible to correct for propagation time. In addition, a proper design of the microstripline and a proper choice of the interrogation power ensure that most of the power is either reflected from or transmitted through a normal zone, and that the absorbed power is small enough that normal zones self-reset.

## VI. CONCLUSION

We have integrated a superconducting meander detector with a commercial MALDI-TOF mass spectrometer and a closed cycle cryocooler, yielding a system with essentially the same footprint as the original spectrometer. The superconducting detector is interfaced directly to the existing spectrometer electronics, allowing use of all the existing software and functionality.

We have also demonstrated the detection efficiency of a Nb meander detector for ions up to  $\sim 200\text{ kDa}$ , the limit of our spectrometer. Despite having an active area approximately 2000 times smaller, the detector produces spectral resolution approaching that of a standard microchannel plate, with improved sensitivity at higher masses.

## ACKNOWLEDGMENT

The authors thank Jason Blumenkamp of JBI Scientific Services for his assistance and expertise with the mass spectrometry system.

## REFERENCES

- [1] G. Siuzdak, "The emergence of mass spectrometry in biochemical research," *Natl. Acad. Sci. USA*, vol. 91, pp. 11290–11297, 1994.
- [2] D. P. Ferguson *et al.*, "Reagentless detection and classification of individual bioaerosol particles in seconds," *Anal. Chem.*, vol. 76, pp. 373–378, 2004.
- [3] D. Twerenbold *et al.*, "Single molecule detector for mass spectrometry with mass independent detection efficiency," *Proteomics*, vol. 1, no. 1, pp. 66–69, 2001.
- [4] D. Twerenbold, J. Vuilleumier, D. Gerber, A. Tadsen, B. Brandt, and P. Gillevet, "Detection of single macromolecules using a cryogenic particle detector couple to a biopolymer mass spectrometer," *Appl. Phys. Lett.*, vol. 28, no. 24, pp. 3503–3505, 1996.
- [5] M. Frank, S. E. Labov, G. Westmacott, and W. H. Benner, "Energy-sensitive cryogenic detectors for high-mass biomolecule mass spectrometry," *Mass Spec. Rev.*, vol. 18, pp. 155–186, 1999.
- [6] M. Frank, "Mass spectrometry with cryogenic detectors," *Nucl. Instr. And Meth. A*, vol. 444, pp. 375–385, 2000.
- [7] M. Ohkubo *et al.*, "Fragmentation analysis by superconducting ion detectors in matrix-assisted laser desorption/ionization (MALDI)," *Nucl. Instr. and Meth. A*, vol. 559, pp. 779–781, 2006.
- [8] G. C. Hilton, J. M. Martinis, D. A. Wollman, K. E. Irwin, L. L. Dulcie, D. Gerber, P. M. Gillevet, and D. Twerenbold, "Impact energy measurement in time-of-flight mass spectrometry with cryogenic microcalorimeters," *Nature*, vol. 391, Feb. 1998.
- [9] K. Suzuki, S. Miki, S. Shiki, Z. Wang, and M. Ohkubo, "Time resolution improvement of superconducting NbN stripline detectors for time-of-flight mass spectrometry," *Appl. Phys. Express*, vol. 1, no. 3, Mar. 2008.
- [10] S. Pagano, E. Esposito, M. Ejrnaes, C. Nappi, and R. Cristiano, "Kinetic inductance detectors for mass spectroscopy," *IEEE Trans. Appl. Supercond.*, vol. 15, no. 2, pp. 940–943, 2005.
- [11] A. J. Kerman *et al.*, "Kinetic-inductance-limited reset time of superconducting nanowire photon counters," *Appl. Phys. Lett.*, vol. 88, p. 111116, 2006.